Limnol. Oceanogr., 48(1), 2003, 290–298

Using natural distributions of short-lived radium isotopes to quantify groundwater discharge and recharge

James M. Krest[1] *and Judson W. Harvey*
U.S. Geological Survey, 430 National Center, 12201 Sunrise Valley Drive, Reston, Virginia 20192

Abstract

Radium activity in pore water of wetland sediments often differs from the amount expected from local production, decay, and exchange with solid phases. This disequilibrium results from vertical transport of radium with groundwater that flows between the underlying aquifer and surface water. In situations where groundwater recharge or discharge is significant, the rate of vertical water flow through wetland sediment can be determined from the radium disequilibrium by a combined model of transport, production, decay, and exchange with solid phases. We have developed and tested this technique at three sites in the freshwater portion of the Everglades by quantifying vertical advective velocities in areas with persistent groundwater recharge or discharge and estimating a coefficient of dispersion at a site that is subject to reversals between recharge and discharge. Groundwater velocities (v) were determined to be between 0 and -0.5 cm d^{-1} for a recharge site and 1.5 ± 0.4 cm d^{-1} for a discharge site near Levee 39 in the Everglades. Strong gradients in ^{223}Ra and ^{224}Ra usually occurred at the base of the peat layer, which avoided the problems of other tracers (e.g., chloride) for which greatest sensitivity occurs near the peat surface—a zone readily disturbed by processes unrelated to groundwater flow. This technique should be easily applicable to any wetland system with different production rates of these isotopes in distinct sedimentary layers or surface water. The approach is most straightforward in systems where constant pore-water ionic strength can be assumed, simplifying the modeling of radium exchange.

The interface between groundwater and surface water is a zone where the interactions between physical, chemical, and biological processes enhance rates of biogeochemical cycling (e.g., Martens 1987; Wersin et al. 1991; Cirmo and McDonnell 1997; Siegel et al. 2001). In marine environments, radium isotopes have been used to quantify water and solute fluxes through this reaction zone by modeling diffusion across the interface (e.g., Hancock et al. 2000; Nozaki et al. 2001), bioturbation (e.g., Cochran 1980; Sun and Torgersen 2001), tidal flushing of the sediments (e.g., Webster et al. 1994; Rama and Moore 1996), or groundwater discharge (e.g., Moore 1997; Krest et al. 2000; Burnett et al. 2002). ^{223}Ra and ^{224}Ra, with their short half-lives (Table 1), promise to be useful for quantifying rates of exchange over short timescales, as occurs in this reaction zone, but only a few studies have examined the geochemistry of these isotopes in groundwater or pore water (e.g., Webster et al. 1994; Hancock et al. 2000; Sun and Torgersen 2001). Several recent studies have used these isotopes to model coastal or estuarine residence times (Moore 2000; Charette et al. 2001; Kelly and Moran 2002), but many questions remain concerning the processes that control the distribution of radium in these systems. For example, the distribution of radium isotopes in the pore water is often not examined, but might be crucial to determining magnitudes and patterns of groundwater radium discharge or recharge. This is particularly true if there is a salinity gradient present that would affect the partitioning of radium between the dissolved and adsorbed phases (Webster et al. 1995; Moore 1999). If we are to utilize these powerful tracers of water flow in biogeochemically complex systems like estuaries and the coastal ocean, we need to make sure we understand what happens as these isotopes are transported through the reaction zone into the surface water. One place to gain understanding of the reaction zone geochemistry of radium is in freshwater wetlands, where pore-water geochemistry is not complicated by large variations in pore-water salinity.

In freshwater systems such as streams and wetlands, groundwater discharge or recharge and hyporheic exchange between surface water and pore water of streambed sediments are important controls on biogeochemical cycling (Grimm and Fisher 1984; Brunke and Gosner 1997; Cirmo and McDonnell 1997; Mulholland et al. 1997; Drexler et al. 1999). ^{223}Ra and ^{224}Ra could be useful for measuring the rate of this exchange, but little work has been reported in which these isotopes have been used as tracers of water flow in freshwater (Kraemer and Genereux 1998) and none that we know of in freshwater wetlands. Although dissolved radium activities are low in most freshwater systems (King et al. 1982; Moore 1999), using radium to determine groundwater exchange in a freshwater system is potentially less problematic than in estuarine or marine systems, where variable pore-water ionic strengths affect sediment-dissolved partitioning coefficients.

[1] Corresponding author (jmkrest@usgs.gov).

Acknowledgments

J. Jackson, J. Choi, and E. Nemeth assisted with sample collection. S. Krupa of the South Florida Water Management Department provided logistical support for our field efforts. In the laboratory, E. Nemeth, K. Randle, and C. Roland assisted with analyses. T. Kraemer and G. Jolly provided radon production rate measurements and lab space for other analyses. M. Doughten assisted with dissolved ion analyses. P. Swarzenski, J. Cable, D. Siegel, and an anonymous reviewer provided comments that helped to improve the manuscript.

Funding from the U.S. Geological Survey's National Research Program and Place-Based Studies Program, and from the South Florida Water Management District supported this research. This work was performed while J.M.K. held a National Research Council Research Associateship Award at the U.S. Geological Survey.

Table 1. Isotopes of interest with their half-lives and decay constants.

Isotope	Half-life	Decay constant (d^{-1})
^{228}Th	1.91 yr	9.94×10^{-4}
^{224}Ra	3.66 d	1.89×10^{-1}
^{227}Ac	21.8 yr	8.72×10^{-5}
^{227}Th	21.7 d	3.70×10^{-2}
^{223}Ra	11.4 d	6.06×10^{-2}

Our freshwater study area, the Florida Everglades, is similar to many estuarine and coastal marine wetlands in that groundwater/surface-water exchange is attenuated by a thin (typically ~1 m thick or less), organic-rich sediment that exists in an almost continuous layer across much of the system. This layer has a lower hydraulic conductivity than underlying sediments, thereby impeding exchange between the surface water and surficial aquifer (Harvey et al. 2002). In other systems, this impeding layer can be of different lithology, but in the Everglades, it is a layer of peat primarily composed of decaying roots and stems of emergent macrophytes. Although vertical water transport does occur across the Everglades peat layer, rates are slow enough that they are difficult to quantify, largely because of very weak hydraulic gradients in most areas of the Everglades (Nemeth et al. 2000). Even modest rates of vertical transport, however, become significant to Everglades water budgets because they often occur over a large area (Choi and Harvey 2000). Common methods for measuring exchange across the peat layer are prone to complications: small hydraulic gradients are difficult to measure over short vertical distances; seepage meters tend to be imprecise at slow rates; radon profiles or emanation rates are complicated by methane bubble ebullition; and chloride profiles commonly exhibit a strong gradient only at the surface of the peat and are affected by other processes (e.g., bubble ebullition) in addition to recharge and discharge.

We present here a method to quantify these slow vertical fluxes through the peat layer by modeling the pore-water profiles of ^{223}Ra and ^{224}Ra. The approach used was to collect field data on natural distributions and production rates of radium in vertical profiles through Everglades peat and to model that data using one-dimensional advective flow models.

Methods

Study site—Site S10C-N is located in the Water Conservation Area-1 (WCA-1), approximately 200 m north of control structure S10-C on Levee 39, also referred to as the Hillsboro levee (Fig. 1). Site S10C-S is located approximately 50 m south of the tailwater canal on the south side of Levee 39, in Water Conservation Area-2A (WCA-2A). Because of water conservation practices, a difference in water level of ~0.3–1 m often occurs between these two sites. As a result of this potentiometric head difference, groundwater recharge is known to occur at S10C-N and groundwater discharge is known to occur at S10C-S (Harvey et al. 2002). Site U3 is located in the interior of WCA-2A, 12 km away from the levee, and the head difference at the levee has a much smaller effect on the groundwater movement at this site. Harvey et al. (2002) showed that the long-term average vertical flux of groundwater at site U3 is small

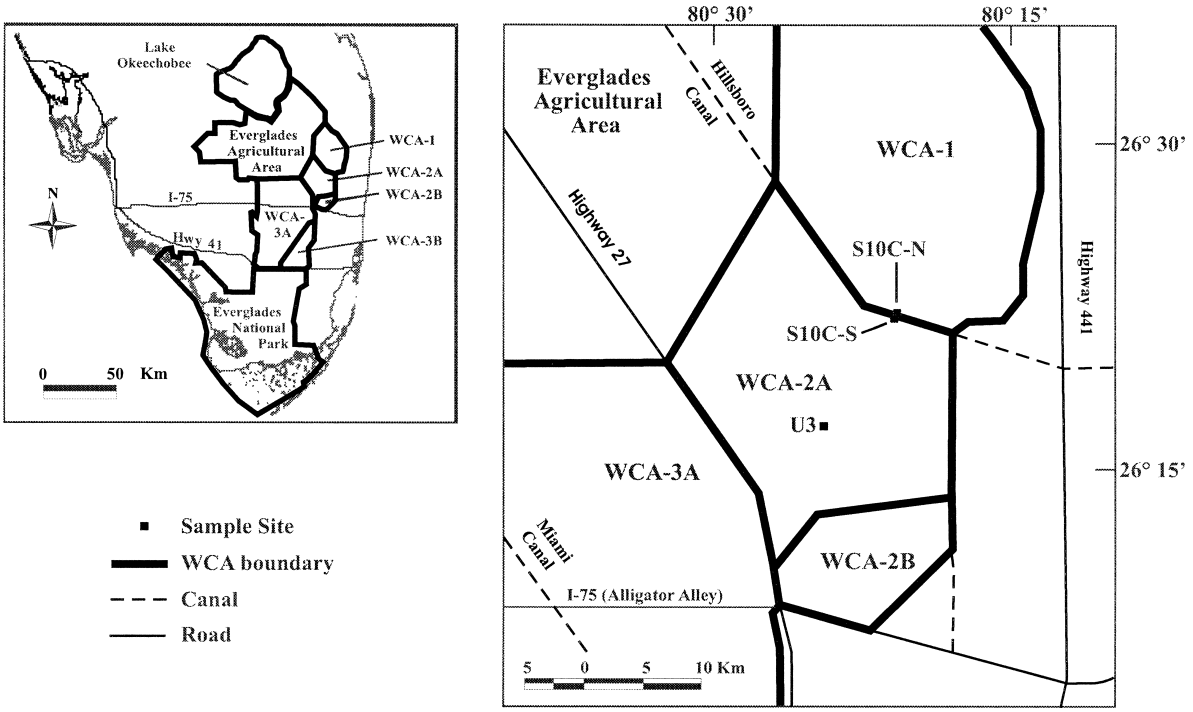

Fig. 1. Map showing the location of sites S10C-N, S10C-S, and U3.

($\sim$0.06 cm d^{-1}), though instantaneous rates can sometimes be as large as $\pm$0.5 cm d^{-1}.

Samples were collected from sites S10C-N and S10C-S on 5 April 2001 and 30 April 2001. Samples were collected from site U3 on 25 September 2001. All sites are in undisturbed sediment and vegetation. The peat layer is approximately 1 m thick at these sites, and the bottom of the peat is well defined with either carbonate or siliceous sediments lying directly beneath it. Above the peat is an unconsolidated detrital layer, commonly called the ''floc'' layer, which is easily disturbed and resuspended into the overlying surface water.

Measurements of dissolved radium—Temporary wells were installed at various depths in the sediments to collect water for measurements of dissolved radium. These wells consisted of either (1) 3/8-inch (0.95 cm) stainless steel drivepoints with vertical slots near the bottom end measuring 0.010 inch (0.025 cm) wide and 2 cm in length or (2) 1/2-inch (1.27 cm i.d.) schedule-40 polyvinyl chloride (PVC) pipes with 5 cm of slotted screen (0.010 inch) near the bottom. The wells were installed in an array to sample at 10–20 cm vertical resolution, making sure that the screened sampling intervals of individual wells were no closer than 50 cm from each other in any direction. Between 0.5 and 2 liters of pore water was pumped at rates $<$100 ml min^{-1} and filtered through 0.45-μm (actual) pore size filters, then passed through Mn-fiber to concentrate the radium isotopes (Moore 1976). ^{223}Ra and ^{224}Ra were analyzed by delayed coincidence counting of the Mn-fiber (Moore and Arnold 1996). Subsamples of the filtered water were also analyzed for chloride by ion chromatography.

Radium distribution—In saturated sediments, a significant fraction of exchangeable radium is dissolved, but most is adsorbed to particles. This partitioning is commonly described as a simple, linear, sorption isotherm ($Ra_{Adsorbed} = K_D \times Ra_{Dissolved}$), which can be rearranged to solve for K_D, the Ra distribution coefficient.

$$K_D = \frac{[Ra_{Adsorbed}]}{[Ra_{Dissolved}]} \quad (1)$$

$Ra_{Adsorbed}$ is the mass of radium per gram dry weight of peat and $Ra_{Dissolved}$ is the mass of radium per mass of pore water.

K_D is often measured in the laboratory either by leaching the exchangeable radium from the sediment using high-ionic strength solutions, or by adding a radium spike or tracer to a sediment slurry and determining the amount taken up in the liquid and solid fractions (e.g., Rama and Moore 1996; Krest et al 1999). However, by treating a sample with dilute hydrogen peroxide, Rama and Moore (1996) demonstrated that oxidation of the sediment during transport and analysis might free up binding sites in the sediment and artificially increase the value of K_D. Sun and Torgersen (1998) provided an improvement on these methods whereby the dissolved and adsorbed phases are quickly separated and measured directly from the water or solid, but some oxidation of the sample can still occur before separation unless great care is taken.

Because of the low radium activities in the Everglades' peat sediments and pore water, K_D could not be measured with good precision using Sun and Torgersen's (1998) method. Instead, K_D was determined for each site by dividing the production rate of the exchangeable radium by the dissolved radium activity according to Eq. 1. This calculation was performed only on data from upper portions of the peat cores, where an equilibrium relationship between the production rate and dissolved activity was demonstrated. Because the dissolved fraction is collected in situ and the production measurement gives total exchangeable radium, oxidation problems are not a concern with this method.

Sediment analyses—Sediment cores 10.2 cm in diameter were taken at each site for measurements of radium production rates, porosity, and dry bulk density. Cores were sectioned in 5- or 10-cm intervals, and interval depths were corrected for compression as measured at the time of coring. Each interval was homogenized, and one fraction was taken to determine the average density of the sediment particles, the average porosity, and the dry bulk density (Lambe 1951). Another fraction of sediment was aged to ensure equilibrium between the radium isotopes and their respective parents, dried, disaggregated in a blender, and analyzed for the production rates of exchangeable ^{223}Ra and ^{224}Ra by delayed coincidence counting of the remoistened sediment (Sun and Torgersen 1998).

Models of vertical transport through peat—Background: The peat layer has different production rates for ^{223}Ra and ^{224}Ra than the surface water or underlying sediments, so profiles of the isotopes near the upper or lower interface can be modeled to determine the advective or dispersive flux across the interface. Water that crosses the interface from one layer to the next will initially have a radium concentration greater than or less than that supported by the local production rate, and as that water parcel continues to travel through the new layer, this dissolved concentration will eventually come into equilibrium with the new production rate. Similarly, at the surface of the peat, profiles can be used to determine the gain or loss due to groundwater recharge if the surface-water activities are different from the supported radium activities in the pore water.

The one-dimensional advection and dispersion models presented below are an appropriate simplification for freshwater systems of the detailed one-dimensional, advective-diffusive transport model recently formulated by Sun and Torgersen (2001). Because of the estuarine system they were working in, their model required considerations for changes in the adsorbed/dissolved radium partitioning coefficient (K_D) and a subjective assignment of separate zones of physical and biological mixing without explicit correlation to pore-water geochemistry or sediment morphology.

Model derivation: ^{223}Ra and ^{224}Ra are produced from the decay of their respective thorium parents. Thorium is extremely particle reactive ($K_D = 10^4$–10^5), so the primary source of these radium isotopes is in and on sediment surfaces. Because radium is much less particle reactive than thorium ($K_D \approx 10^2$–10^3 in freshwater), an appreciable fraction is dissolved in pore water. As a dissolved ion, radium

is transported with pore fluids, and its gain or loss near sediment/sediment or sediment/water interfaces can be modeled in saturated sediments as a balance of its production, decay, advection, dispersion, and exchange with particles (Berner 1980).

$$\frac{dC}{dt} = \mathrm{D}\frac{\partial^2 C}{\partial Z^2} - v\frac{\partial C}{\partial Z} + \frac{\hat{P}\rho}{f\mathrm{K_D} + (1 - f)} - \lambda C + \frac{\partial C^*}{\partial t}\frac{\rho}{\mathrm{K_D}} \quad (2)$$

where t is time, Z is depth below the peat surface, C is the number of dissolved radium atoms per volume of water, C^* is the number of adsorbed radium atoms per mass of dry sediment, D is the hydrodynamic dispersion coefficient in units of (length)^2 per time, v is the pore-water advective velocity in units of length per time, $\hat{P}$ is the production rate of exchangeable radium (dissolved plus adsorbed) from its respective parent isotope in atoms per time, per mass of bulk sediment, ρ is the pore water density in mass per volume, f is the mass of dry sediment per mass of bulk sediment, $\mathrm{K_D}$ is the radium distribution coefficient (Eq. 1), and λ is the respective decay constant (0.189 d^{-1} for ^{224}Ra; 0.0606 d^{-1} for ^{223}Ra).

When conditions are at steady state, and in areas where advective fluxes greatly exceed dispersive fluxes, Eq. 2 can be simplified and solved for the concentration of radium at any depth in the peat ($C(Z)$).

$$C(Z) = P\lambda^{-1} + (C_\mathrm{I} - P\lambda^{-1})e^{-\Delta Z\lambda v^{-1}} \quad (3)$$

Here, C_I is the radium concentration at an interface defined by the investigators as the depth of a transition between sedimentary layers or the depth of the sediment/surface-water interface. ΔZ is calculated as the difference between the depth of the interface and the sample depth so that $\Delta Z = 0$ at the interface and is positive upward. The boundary conditions are $C(\Delta Z = 0)$ is equal to the measured C_I, and $C(\Delta Z = \infty)$ is equal to P. P is equal to $\hat{P}/(f\mathrm{K_D} + (1 - f))$—the fraction of the exchangeable radium production that will enter the pore water—and is analogous to the supported, dissolved radium activity at equilibrium.

In some areas of the Everglades, vertical velocities are slow and often reverse directions so that the average advective velocity approaches zero (Harvey et al. 2002). In these areas, it might be more appropriate to model dispersion as the dominant transport process. The steady-state solution to Eq. 2 for the case where dispersion dominates over advection is shown in Eq. 4.

$$C(Z) = P\lambda^{-1} + (C_\mathrm{I} - P\lambda^{-1})e^{-|\Delta Z|\lambda^{0.5}\mathrm{D}^{-0.5}} \quad (4)$$

The absolute value of the distance from the interface ($|\Delta Z|$) is needed in Eq. 4 to allow for the most general case where ΔZ could be a positive or negative distance from the interface in this coordinate system.

It would have been preferable to solve for advection and dispersion simultaneously, but at very low pore-water velocities, it is unlikely that analytical uncertainties will allow us to separate these variables. At low velocities, the advective and dispersive terms are usually similar in magnitude, and if both terms are included, they occur as a ratio in the solution and cannot be independently estimated. Indeed, model curves produced from Eqs. 3 and 4 are nearly identical, and the choice of one over the other depends primarily on our knowledge of the hydraulics and geochemistry of the system.

It must be noted that the radium production rate has been described as a constant through the sediment layer being studied. In relatively homogeneous sediments, this assumption should be valid but should be tested for individual systems. In this freshwater system, we are assuming that $\mathrm{K_D}$ is constant through each layer of sediment as long as we can demonstrate that the ionic strength of the pore water does not change appreciably with depth. Because $\mathrm{K_D}$ is constant and we are modeling for steady-state conditions, retardation of radium is not a factor (Berner 1980; Tricca et al. 2001).

Because radium is generally measured and discussed in terms of its activity (A) rather than its concentration, we multiply both sides of Eqs. 3 and 4 by λ ($A = C\lambda$). The vertical profile of dissolved radium is therefore described by Eqs. 5a and 5b.

$$A(Z) = P + (A_\mathrm{I} - P)e^{-\Delta Z\lambda v^{-1}} \quad \text{(for advection)} \quad (5a)$$

or

$$A(Z) = P + (A_\mathrm{I} - P)e^{-|\Delta Z|\lambda^{0.5}\mathrm{D}^{-0.5}} \quad \text{(for dispersion)} \quad (5b)$$

A_I is the dissolved radium activity at the interface and $A(Z)$ is the dissolved radium activity as a function of depth.

Results

Test of model assumptions—The one-dimensional advective and dispersive transport models defined above require that certain conditions or assumptions be reasonably well met. The principal conditions are that (1) the pore-water radium activity near the sediment/sediment or sediment/surface-water interface is out of balance with the activity that would be expected as a function of the radium production rate in the sediments and the partitioning of radium between the dissolved and adsorbed phase and that this disequilibrium can be described as the result of either advective or dispersive transport across the interface; (2) the sedimentary layers are relatively homogeneous chemically and physically, and the interface between the layers is well defined; (3) the radium production rates are constant through each layer, but significantly different between the two layers; and (4) the partitioning of radium between the dissolved and adsorbed phase is constant through each layer. The first condition we already addressed using our knowledge of the vertical hydraulic gradient in Everglades peat. We will address the remaining three conditions here.

The Everglades' peat layer is relatively homogeneous in bulk sediment properties (Fig. 2a). For example, at site S10C-N porosity of peat is very high (0.93 ± 0.02), the density of peat is relatively low (1.34 ± 0.08 g cm^{-3}), and the dry bulk density of peat is also very low (0.09 ± 0.02 g cm^{-3}). The base of the peat is well-defined and is characterized at all the sites by a distinct change from the high-porosity, low-density peat sediments to high-density, low-porosity silicate or carbonate sediments. The underlying

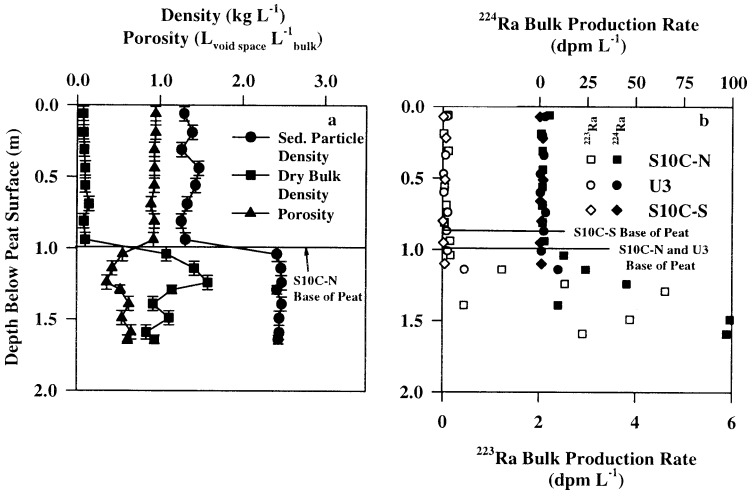

Fig. 2. Physical and chemical characteristics of the sediments. (a) The base of the peat is readily apparent by the decrease in porosity and the increases in the average density of the sediment grains and the dry bulk density at site S10C-N. (b) Production rates of ^{224}Ra and ^{223}Ra are constant through the peat layer, but then increase below the peat. This increase is most apparent in sediment samples taken from a 1.8-m core at site S10C-N where the production rates initially increase exponentially below 0.9 m and then become irregular with variations in sediment lithology (compare with dry bulk density profile in panel a). Solid horizontal lines in panels a and b indicate the base of the peat layers.

silicates or carbonates are reasonably homogeneous in terms of their physical characteristics, but not their chemical characteristics (Fig. 2b). The production rates of ^{223}Ra and ^{224}Ra are constant through the peat layer, but much more variable in the sediments below the peat.

K_D values were determined from the relationship between the exchangeable radium and dissolved radium (Eq. 1). The dissolved radium was approximated as the average of the dissolved radium samples between 10 and 50 cm depth in the peat ($\bar{A}$). Dissolved activities in this interval were all very similar, suggesting equilibrium had been reached between production, decay, and exchange. The total exchangeable radium was estimated from the production rate of the exchangeable radium, again assuming that equilibrium conditions existed for this interval. K_D values ranged from 120 to 280 for the peat sediments (Table 2).

In homogeneous sediments, changes in K_D would most likely result from changes in the ionic strength of the pore water. Because chloride can be measured with much greater precision than K_D, chloride concentration was used as a proxy of ionic strength to test the constancy of K_D in the peat and aquifer sediments. Figure 3a shows chloride concentration as a function of depth, and Fig. 3b shows pore-water radium activity as a function of chloride concentration. There is little or no correlation between chloride concentration and depth or between radium activity and chloride concentration, suggesting that K_D is constant in the peat layer. Unfortunately, we cannot extend this relationship below the base of the peat because of the confounding effects of changing sediment characteristics.

Quantify rates of exchange—Figure 4a,b shows pore-water ^{224}Ra and ^{223}Ra activities in the peat layer at site S10C-S. The activities are highest near the base of the peat as a result of upward transport from below. Activities decrease exponentially to a constant value in the upper portion of the peat as the excess radium decays away and the activity of the dissolved plus adsorbed fraction approaches equilibrium with the production rate. Overlying the data in Fig. 4a,b are model-derived lines for upward advection of radium and pore fluids based on Eq. 5a. For all data sets, the ''best fit'' parameters v or D, A_I, and P were determined using a curve-

Table 2. Radium distribution coefficients (K_D) in Everglades peat. nd, not determined; dpm, disintegrations or atoms per minute.

	S10C-S		210C-N		U3	
	^{224}Ra	^{223}Ra	^{224}Ra	^{223}Ra	^{224}Ra	^{223}Ra
$\hat{\bar{P}}$ (dpm kg^{-1})	21.2	0.49	25.5	0.66	34.9	0.91
$\bar{A}$ (dpm [100 L]$^{-1}$)*	8.42	0.34	10.2	0.29	20.2	0.55
P (dpm [100 L]$^{-1}$)†	7.60	0.40	nd	nd	17.0	0.60
K_D (using $\bar{A}$)	250	144	250	230	170	160
K_D (using P)	280	120	nd	nd	210	150

* $\bar{A}$ is the average of the dissolved radium activities between 10 and 50 cm in the peat.
† The value for P is determined from the model (*see text* and Table 3).

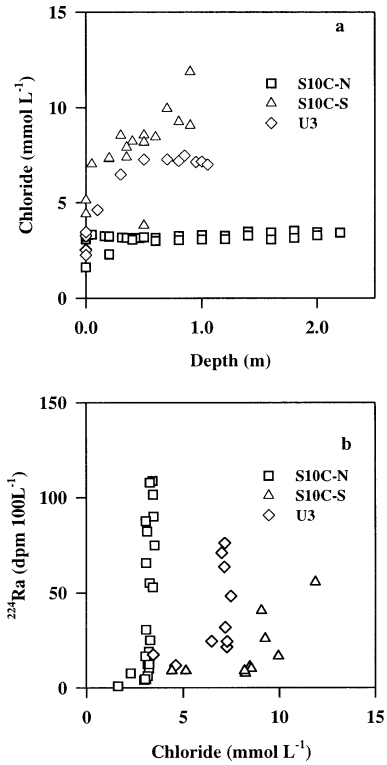

Fig. 3. (a) Concentrations of dissolved chloride are plotted as a function of depth to show the lack of variation through the peat and underlying sediment. (b) ^{224}Ra shows no correlation with chlorinity below a few centimeters in the core, supporting the assumption that K_D is constant through the homogeneous sediment layers (*see text*). The trend for ^{223}Ra is similar and is not shown here.

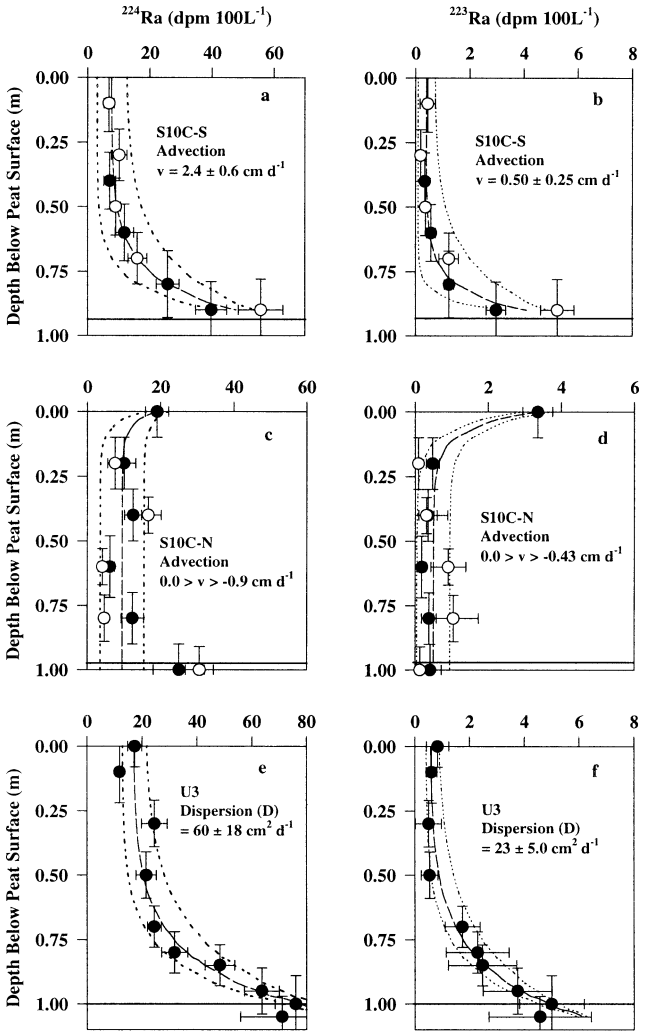

Fig. 4. Pore-water radium activities as a function of depth. (a) ^{224}Ra and (b) ^{223}Ra activities at site S10C-S are highest at the base of the peat, indicated by a solid horizontal line, and decrease upward as the excess radium in discharging groundwater decays to a level supported by its equilibrium production and exchange with the adsorbed fraction. (c) ^{224}Ra and (d) ^{223}Ra activities at S10C-N are elevated only in the upper portion of the peat, suggesting that recharge occurs at this site. (e) ^{224}Ra and (f) ^{223}Ra profiles at site U3 are similar to profiles from S10C-S but have been modeled for dispersive transport because of independent observations that recharge and discharge alternate at this site. Model curves in panels a, b, e, and f indicate the best fit to the data along with 95% confidence intervals based on the uncertainty of the three parameters (v or D, A_I, and P). The central model curves in panels c and d indicate the upper limit of our estimate for the magnitude of the recharging velocity (v) with the best estimate for the boundary conditions, A_I and P. The outer model curves in panels c and d use the same value for v as the central line and their spread is based on the analytical uncertainty of the boundary conditions.

fitting routine that maximized the log of the likelihood function using a Nelder–Mead simplex algorithm and assuming a Poisson distribution. The center line in each panel of Fig. 4 shows the best fit simulation, modeled using the parameters identified by the fitting routine. The two outside lines indicate the 95% confidence intervals (mean ± 2 SE) for combined uncertainty in the velocity or coefficient of dispersion (v or D), radium activity at the interface (A_I), and the production rate in the peat (P). Based on the ^{224}Ra and ^{223}Ra model fits, the advective velocity at site S10C-S is 2.4 ± 0.6 cm d^{-1} or 0.50 ± 0.25 cm d^{-1}, respectively.

Data from site S10C-N are modeled in Fig. 4c,d using Eq. 5a. Activities are nearly constant through the peat but are slightly higher at the very surface of the peat. The activity gradient near the surface and the lack of a gradient at depth, despite an increased production rate in the sand beneath the peat, indicate that groundwater is recharging at this site. Sampling intervals were not adequate to precisely determine the activity gradient at the top of the peat, but model fits are useful to constrain the possible maximum rate of advective transport. The ^{224}Ra profile indicates that magnitude of the recharge is less than 0.9 cm d^{-1}. The ^{223}Ra profile constrains the magnitude of recharge to less than 0.43 cm d^{-1}. Because the radium production rate is not constant in the sediments below the peat, we are unable to further constrain the rate of recharge at site S10C-N by modeling the radium profiles below the peat.

Figure 4e,f shows the result of fitting the dispersive transport model (Eq. 5b) to pore-water ^{224}Ra activities at site U3, resulting in coefficient of dispersion values of 60 ± 18 cm^2

Table 3. Model results and calculated radium fluxes to the surface water. nd, not determined; dpm, disintegrations or atoms per minute.

Site	Model parameter	Model result			Flux (dpm $m^{-2}d^{-1}$)	
		^{223}Ra	^{224}Ra	Average	^{223}Ra	^{224}Ra
S10C-S	v (cm d^{-1})	0.50±0.25	2.4±0.6	1.5±0.4	0.06	1.1
	C_I (dpm [100 L]$^{-1}$)	4.1±0.4	48±3			
	P (dpm [100 L]$^{-1}$)	0.4±0.3	7.6±2.3			
S10C-N	v (cm d^{-1})	−0.43*	−0.9*	−0.43*	nd	nd
	C_I (dpm [100 L]$^{-1}$)	nd	nd			
	P (dpm [100 L]$^{-1}$)	nd	nd			
U3	v (cm d^{-1})	1.2±0.2	3.4±0.5	2.3±0.3	0.14	3.9
	C_I (dpm [100 L]$^{-1}$)	4.9±0.2	77±3			
	P (dpm [100 L]$^{-1}$)	0.6±0.1	17±2			
U3	D (cm^2 d^{-1})	23±5.0	60±18	42±9.3	0.07	4.1
	C_I (dpm [100 L]$^{-1}$)	4.9±0.2	77±4			
	P (dpm [100 L]$^{-1}$)	0.6±0.1	17±2			

* Maximum magnitude (i.e., value $< v < 0$).

d^{-1} and 23 ± 5 cm^2 d^{-1} from ^{224}Ra and ^{223}Ra profiles, respectively. Model results for all sites are summarized in Table 3.

Discussion

The one-dimensional models derived to explain the advective (Eq. 5a) or dispersive (Eq. 5b) transport of short-lived radium isotopes through pore water are based on a number of implicit assumptions. It is important to keep in mind that these simple models require the radium production rate and the radium distribution coefficient (K_D) to be constant through the sediment layer being studied. If these assumptions are not met, more detailed geochemical terms will be needed in the governing equation to account for these additional complexities (e.g., Cochran 1980; Sun and Torgersen 2001).

Testing the assumption of constant radium production was simplified recently by Sun and Torgersen's (1998) elegant method of measuring the emanation of ^{220}Rn from a column of moistened sediment to determine the amount of exchangeable ^{224}Ra in the sample. This method quickly and easily determines the amount of ^{224}Ra adsorbed to the sediment particles, and this surface-bound radium is the fraction subjected to the processes of adsorption, desorption, and transport in the dissolved phase. Using samples that have been aged to ensure ^{224}Ra is in equilibrium with its ^{228}Th parent allows us to determine the production rate of surface-bound ^{224}Ra. We also determined the production rate of the surface-bound ^{223}Ra in the peat samples by applying the same theory to the ^{227}Ac–^{223}Ra–^{219}Rn decay series. Figure 2b shows that the ^{223}Ra and ^{224}Ra production rates are constant through the peat layer but become more variable in the deeper sediments. Our assumptions for modeling vertical transport of radium through the peat are therefore reasonable, but variability in production rates below the peat mean that vertical transport in the sand and limestone layers are too complicated to be accurately described by our simplified transport models.

A gradient in the radium distribution coefficient (K_D) could similarly cause an apparent dissolved radium gradient in the pore water. Therefore, good knowledge of K_D through the sediment layer is essential. Sun and Torgersen (1998, 2001) measured K_D directly from the sediment samples and the pore water extracted from the sediment intervals. However, because of the low radium concentrations in the Everglades peat and pore-water samples, our estimates of K_D could be determined experimentally only from certain sediment and pore-water samples collected far enough from the interface to ensure an equilibrium relationship between the dissolved radium and its production rate. There is excellent agreement between the average dissolved radium activity in samples collected away from the interface (A) and the model-derived estimate of the production rate of the dissolved radium (P), giving us confidence that equilibrium has been reached between production, decay, and exchange in this interval (Table 2).

Because of the significant potential for error in estimating K_D in freshwater sediments, small trends of variation in K_D as a function of depth might not be noticed in the data even though they could have large effects on the dissolved radium activities. Because the strongest control on the radium distribution coefficient in homogeneous portions of the sediment is likely to be the ionic strength of the solution (Copenhaver et al. 1993; Webster et al. 1995) and because chloride concentration is the overwhelming contributor to the anion side of the charge balance, the constancy of the chloride concentration with depth was used as a first-order approximation of the constancy of K_D (Fig. 3a).

Furthermore, radium activity shows no correlation to the chloride concentration at any site, except possibly in the most surficial samples at site S10C-S (Fig. 3b). This slight correlation is not of concern in this study because pore-water radium concentrations in the upper part of the peat are all very similar and have little or no bearing on the radium distribution in the bottom of the core where the concentration gradient is being modeled.

Radium profiles at S10C-S are consistent with groundwater discharge, with a modeled advective velocity (averaged for the results of the two radium isotopes) of 1.5 ± 0.7 cm d^{-1}. The model result for the advective velocity is not very sensitive to the boundary conditions; the analytical uncertainty of the radium activity and production rate boundary

conditions adequately cover the spread of radium activities in the pore-water profiles (Fig. 4). An advantage of this model is that the activity gradient being modeled occurs deep within the peat, away from the surface of the peat where mechanical disturbances to the system could easily distort the signal.

The radium profile at site U3 is very similar to the profile at the groundwater discharge site, S10C-S. Fitting the advective transport model to the U3 data results in an advective velocity of 2.3 ± 0.5 cm d^{-1}, which is slightly higher than the velocity calculated for S10C-S, although not statistically different. The issue of whether the primary transport mechanism is advective or dispersive cannot be resolved by measuring the flux to the surface water: for advective transport, the radium flux (J) is roughly calculated as the average radium pore-water activity in the upper part of the core multiplied by the velocity (Berner 1980).

$$J = A \cdot v \tag{6}$$

In the case of dispersion, the maximum flux is a function of the dispersion coefficient and the decay constant (Krest et al. 1999).

$$J = \Delta A \sqrt{D\lambda} \tag{7}$$

ΔA can be approximated in this case as the difference between the pore-water and the surface-water radium activities. On the basis of the values for v and D calculated from the radium pore-water profiles, radium fluxes to the overlying surface water at site U3 should be the same without regard as to whether the primary transport is modeled as a function of advection or dispersion (Table 3).

Modeling the radium pore-water profiles as described in this paper determines limits for the flux of radium to surface water and can be used as an important test in mass balance models for surface-water radium. Furthermore, results of the solution of these one-dimensional vertical models will also be useful for estimating the transport rates of nutrients and other solutes into or out of the pore water and can be used to quantify solute storage and release rates and biogeochemical cycling. One of the key advantages of this technique is that dispersion and upward advection are measured at depth in the sediment column, away from mechanical disturbances to the surficial sediment. In an environment with consistent radium production rates in deeper sediment layers, this advantage would hold true for recharge measurements as well. These techniques can be adapted for any wetland systems that have well-defined layers (sedimentary or sediment/surface-water transition) creating distinct discontinuities in the radium production rate, but they must be used with caution in environments where there are uncertainties in the constancy of lithology or ionic strength within layers. For those situations, more data and a more detailed model representation will be required.

References

BERNER, R. A. 1980. Early diagenesis—a theoretical approach. Princeton Series in Geochemistry, Princeton University Press.

BRUNKE, M., AND T. GOSNER. 1997. The ecological significance of exchange processes between rivers and groundwater. Freshw. Biol. **37:** 1–33.

BURNETT, B., AND OTHERS. 2002. Assessing methodologies for measuring groundwater discharge to the ocean. EOS Trans. Am. Geophys. Union **83:** 117, 122–123.

CHARETTE, M. A., K. O. BUESSELER, AND J. E. ANDREWS. 2001. Utility of radium isotopes for evaluating the input and transport of groundwater-derived nitrogen to a Cape Cod estuary. Limnol. Oceanog. **46:** 465–470.

CHOI, J., AND J. W. HARVEY. 2000. Quantifying time-varying groundwater discharge and recharge in wetlands: A comparison of methods in the Florida Everglades. Wetlands **20:** 500–511.

CIRMO, C. P., AND J. J. MCDONNELL. 1997. Linking the hydrologic and biogeochemical controls of nitrogen transport in near-stream zones of temperate-forested catchments: A review. J. Hydrol. **199:** 88–120.

COCHRAN, J. K. 1980. Radium, thorium, uranium and ^{210}Pb in deep sea sediment and sediment pore waters in the north equatorial Pacific. Am. J. Sci. **280:** 849–889.

COPENHAVER, S. A., S. KRISHNASWAMI, K. K. TUREKIAN, N. EPLER, AND J. K. COCHRAN. 1993. Retardation of U-238 and Th-232 decay chain radionuclides in Long-Island and Connecticut aquifers. Geochim. Cosmochim. Acta **57:** 597–603.

DREXLER, J. Z., B. L. BEDFORD, R. SCOGNAMIGLIO, AND D. I. SIEGEL. 1999. Fine-scale characteristics of groundwater flow in a peatland. Hydrol. Process. **13:** 1341–1359.

GRIMM, N. B., AND S. G. FISHER. 1984. Exchange between interstitial and surface water: Implications for stream metabolism and nutrient cycling. Hydrobiologia **111:** 219–228.

HANCOCK, G. J., I. T. WEBSTER, P. W. FORD, AND W. S. MOORE. 2000. Using Ra isotopes to examine transport processes controlling benthic fluxes into a shallow estuarine lagoon. Geochim. Cosmochim. Acta **64:** 3685–3699.

HARVEY, J. W., AND OTHERS. 2002. Interactions between the surface-water and ground-water and effects on mercury transport in the north-central Everglades. Water-Resources Investigation WRI 02-4050, U.S. Geological Survey.

KELLY, R. P., AND S. B. MORAN. 2002. Seasonal changes in groundwater input to a well-mixed estuary estimated using radium isotopes and implications for coastal nutrient budgets. Limnol. Oceanog. **47:** 1796–1807.

KING, P. T., J. MICHEL, AND W. S. MOORE. 1982. Ground water geochemistry of ^{228}Ra, ^{226}Ra and ^{222}Rn. Geochim. Cosmochim. Acta **46:** 1173–1182.

KRAEMER, T. F., AND D. P. GENEREUX. 1998. Applications of uranium and thorium-series radionuclides in catchment hydrology studies, pp. 679–722. *In* C. Kendall and J. J. McDonnell [eds.], Isotope tracers in catchment hydrology. Elsevier.

KREST, J. M., W. S. MOORE, L. R. GARDNER, AND J. T. MORRIS. 2000. Marsh nutrient export supported by groundwater discharge: Evidence from radium isotope measurements. Glob. Biogeochem. Cycles **14:** 167–176.

———, ———, AND RAMA. 1999. ^{226}Ra and ^{228}Ra in the mixing zones of the Mississippi and Atchafalaya Rivers: Indicators of groundwater input. Mar. Chem. **64:** 129–152.

LAMBE, T. W. 1951. Soil testing for engineers. Series in Soil Engineering, Wiley.

MARTENS, C. S. 1987. Processes at the sediment–water interface—advances during 1982–1986. Rev. Geophys. **25:** 1421–1426.

MOORE, W. S. 1976. Sampling ^{228}Ra in the deep ocean. Deep-Sea Res. **23:** 647–651.

———. 1997. High fluxes of radium and barium from the mouth of the Ganges–Brahmaputra river during low river discharge suggest a large groundwater source. Earth Planet. Sci. Lett. **150:** 141–150.

———. 1999. The subterranean estuary: A reaction zone of ground water and sea water. Mar. Chem. **65:** 111–125.

———. 2000. Ages of continental shelf waters determined from ^{223}Ra and ^{224}Ra. J. Geophys. Res. **105:** 22,117–22,122.

———, AND R. ARNOLD. 1996. Measurement of Ra-223 and Ra-224 in coastal waters using a delayed coincidence counter. J. Geophys. Res. Oceans **101:** 1321–1329.

MULHOLLAND, P. J., E. R. MARZOLF, J. R. WEBSTER, D. R. HART, AND S. P. HENDRICKS. 1997. Evidence that hyporheic zones increase heterotrophic metabolism and phosphorus uptake in forest streams. Limnol. Oceanogr. **42:** 443–451.

NEMETH, M. S., W. M. WILCOX, AND H. M. SOLO-GABRIELE. 2000. Evaluation of the use of reach transmissivity to quantify leakage beneath Levee 31N, Miami–Dade County, Florida. Water-Resources Investigations Report WRIR 00-4066, U.S. Geological Survey.

NOZAKI, Y., Y. YAMAMOTO, T. MANAKA, H. AMAKAWA, AND A. SNIDVONGS. 2001. Dissolved barium and radium isotopes in the Chao Phraya River estuarine mixing zone in Thailand. Cont. Shelf Res. **21:** 1435–1448.

RAMA, AND W. S. MOORE. 1996. Using the radium quartet for evaluating groundwater input and water exchange in salt marshes. Geochim. Cosmochim. Acta **60:** 4645–4652.

SIEGEL, D. I., J. P. CHANTON, P. H. GLASER, L. S. CHASAR, AND D. O. ROSENBERRY. 2001. Estimating methane production rates in bogs and landfills by deuterium enrichment of pore water. Glob. Biogeochem. Cycles **15:** 967–976.

SUN, Y., AND T. TORGERSEN. 1998. Rapid and precise measurement method for adsorbed ^{224}Ra on sediments. Mar. Chem. **61:** 163–171.

———, AND ———. 2001. Adsorption–desorption reactions and bioturbation transport of ^{224}Ra in marine sediments: A one-dimensional model with applications. Mar. Chem. **74:** 227–243.

TRICCA, A., G. J. WASSERBURG, D. PORCELLI, AND M. BASKARAN. 2001. The transport of U- and Th-series nuclides in a sandy unconfined aquifer. Geochim. Cosmochim. Acta **65:** 1187–1210.

WEBSTER, I. T., G. J. HANCOCK, AND A. S. MURRAY. 1994. Use of radium isotopes to examine pore-water exchange in an estuary. Limnol. Oceanog. **39:** 1917–1927.

———, ———, AND ———. 1995. Modeling the effect of salinity on radium desorption from sediments. Geochim. Cosmochim. Acta **59:** 2469–2476.

WERSIN, P., P. HOHENER, R. GIOVANOLI, AND W. STUMM. 1991. Early diagenetic influences on iron transformations in a freshwater lake sediment. Chem. Geol. **90:** 233–252.

Received: 19 June 2002
Accepted: 15 October 2002
Amended: 17 October 2002